Phase noise mitigation of the microwave-to-photonic conversion process using feedback on the laser current

DAMIEN TEYSSIEUX[1], RODOLPHE BOUDOT[*,1], CHRISTOPHE FLUHR[2], AND JACQUES MILLO[1]

[1] FEMTO-ST, CNRS, UBFC, ENSMM, 26 chemin de l'Epitaphe 25030 Besançon Cedex, France
[2] FEMTO Engineering, 15B avenue des Montboucons, 25030 Besançon Cedex, France
[*] Corresponding author: rodolphe.boudot@femto-st.fr

Compiled October 10, 2022

The generation and transfer of ultra-stable microwave signals is of paramount importance in numerous applications spanning from radar systems, communications and metrology. We demonstrate residual phase noise mitigation at 10 GHz of a directly-modulated laser system through active control of the laser bias current. The latter is tuned to a finely selected point, where the current-to-phase dependence, measured at several microwave power and frequency values, is maximized. A residual phase noise of -113 dBrad^2/Hz at 1 Hz offset frequency from a 10 GHz carrier, with a fractional frequency stability of 1.2×10^{-16} at 1 s and below 10^{-19} at 10^5 s, are measured. These performances are compliant with the transfer of the most stable microwave signals available to date, obtained with cryogenic sapphire oscillators or combs locked to cavity-stabilized lasers. This approach is of interest for the distribution of ultra-stable microwave signals in a very simple photonic configuration.

OCIS codes: (120.3930) Metrological instrumentation; (120.0120)Instrumentation, measurement, and metrology; (250.0250) Optoelectronics; (140.0140) Lasers and laser optics;

http://dx.doi.org/10.1364/ao.XX.XXXXXX

1. INTRODUCTION

Ultra-stable and high-spectral purity microwave signals are of strategic interest in a relevant number of applications and technologies, including Doppler and chirp radars for which the echo signal should not be obscured by the oscillator noise sidebands [1], communications with reduced bit error rate and enhanced security [2], the development of state-of-the-art microwave atomic clocks [3], high-precision synchronization systems [4], signal measurement instrumentation [5] or radio-astronomy using very-long base line intererometry (VLBI) [6].

The majority of currently-deployed low noise microwave sources rely on room-temperature frequency-multiplied quartz crystal oscillators [7], sapphire oscillators [8, 9], or opto-electronic [10, 11] and Brillouin-based oscillators [12]. These systems exhibit excellent phase noise for offset frequencies higher than 1 kHz but are not adapted to support stringent close-to-carrier noise specifications required for quantum sensing [13], Doppler radar systems with slow-moving objects or high density communications.

To date, some of the most stable microwave signals are delivered by cryogenic sapphire oscillators (CSOs). These machines, now robust, mature and commercially-available, provide 10 GHz signals with phase noise levels below -100 dBrad^2/Hz at 1 Hz offset frequency [14–16], motivating their growing dissemination in metrology laboratories as local oscillators for atomic fountain clocks. Nevertheless, CSOs usually exhibit a modest phase noise floor, induced by the thermal noise floor of the sustaining loop microwave amplifiers [17].

The purest microwave signals have been achieved by frequency-dividing the optical wave of ultra-narrow linewidth cavity-stabilized lasers to the microwaves domain using optical frequency combs [18–20]. Best systems offer microwave signals with phase noise levels of -103 and -180 dBrad^2/Hz at 1 Hz and 100 kHz offset frequencies, respectively [18–21]. Some substantial efforts have also been pursued towards the use of the transfer oscillator technique [21, 22], the use of monolithic free-running combs [23] or the development of chip-scale microresonator combs [24, 25].

Once generated, ultra-stable microwave signals have to be disseminated for end users. In this domain, the use of optical fiber links [26–28], that benefit from low losses and already-implemented infrastructures, has shown a remarkable progress [29–32], with the recent demonstration of microwave frequency

Fig. 1. Experimental set-up for basic characterizations of current-to-phase dependence. DFB: Distributed feedback laser. VOA: voltage-controlled optical attenuator. FPD: fast photodiode. The length of fiber patches is about 1 m.

transfer reaching resolution and stability levels in the 10^{-18} range for links of hundreds of kilometers [33, 34].

The photonic transfer of a microwave signal relies on two main steps. In the first step, an optically-carried microwave reference is obtained, through direct current modulation [31, 35] or external modulation with an electro-optic modulator [29, 32, 33] of a laser source. In a second step, this microwave signal is transferred from a point to another through an optical fiber link at the output of which is placed a fast photodiode and amplification, for microwave extraction.

In such a system, the phase of the optically-carried microwave signal can be perturbed by vibrations, stress or temperature fluctuations along the fiber path. Numerous studies have been then performed to mitigate these phase perturbations though the implementation of advanced compensation techniques [27, 31]. At the opposite, phase perturbations induced by the microwave-photonic conversion process itself (laser modulation), treated in some model studies [36–38], are more rarely considered. Yet, this contribution can become a possible limitation, especially when low flicker phase noise signals are treated. In addition, special care must be taken to implement the photodetection and amplification stage used to recover the microwave signal.

In this paper, we demonstrate mitigation of the residual microwave phase noise, induced by the microwave-photonic conversion process, of a directly-modulated laser. In this method, the phase of the optically-carried microwave signal, extracted with a fast photodiode, is measured though a heterodyne setup with a microwave mixer and suppressed through a feedback loop by changing the bias current of the diode. The effect of the bias current on the optically-carried microwave signal phase was studied for a large range of microwave powers and frequencies. A residual phase noise of $-$ 113 dBrad^2/Hz at 1 Hz offset from a 10 GHz carrier is obtained. The fractional frequency stability is measured to be 1.2×10^{-16} at 1 s and below 10^{-19} at 10^5 s. These performances are compliant with the transfer of state-of-the-art microwave signals in a simple configuration.

2. EXPERIMENTAL SETUP AND CHARACTERIZATION

Figure 1 shows the setup used to characterize the impact of the laser bias current onto the phase of the optically-carried microwave signal. The laser source is a single-mode pigtailed distributed feedback (DFB) diode laser (Gooch and Housego AA0701), with internal isolator, that emits at a wavelength of about 1550 nm. The diode laser is integrated in a metallic package that contains a thermo-electric cooler and a thermistor, and is driven by a low noise current controller based on the Libbrecht-Hall design [39]. We measured for this laser a threshold current of about 10 mA and a slope efficiency at 25°C of about 0.19 W/A, yielding about 16 mW of output optical power at a bias current I_{bias} of 90 mA. The 10 GHz signal of a microwave synthesizer is

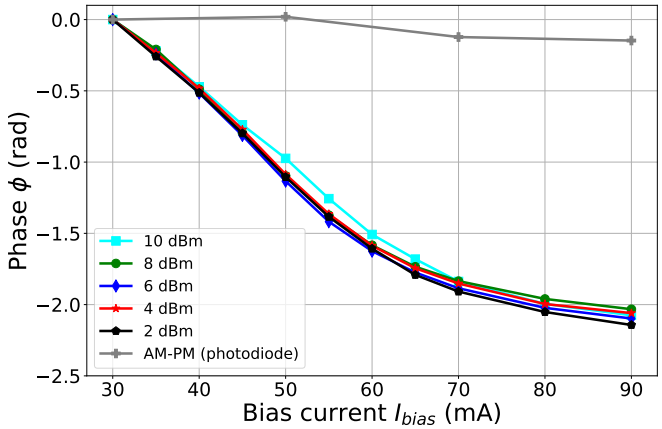

Fig. 2. Phase ϕ of the optically-carried microwave signal, at point B, versus the bias current of the diode laser, at a microwave frequency of 10 GHz, for several microwave power values at the laser input (point A). The contribution to the measured phase variation of the AM-PM conversion process in the photodiode is reported. The reference phase value was arbitrarily fixed to 0 for the lowest tested bias current value.

split into two paths. The first arm (node A) is directly sent into the input channel of a fast oscilloscope (sampling rate: 80 GS/s, acquisition time: 5 ns). In the second arm, the microwave signal is sent into the microwave input of the diode laser through a DC block (not shown on figure 1). The fiber output of the diode laser is connected to a variable optical attenuator (VOA, IDIL COCOM03898) used to control the total optical power and sent to a fast photodiode (Discovery DSC30). The photodiode is operated at a bias voltage of 5 V. The 10 GHz signal extracted at the photodiode output is then amplified by four amplifiers (Hittite HMC606, total gain of 46 dB) and sent to a second channel of the oscilloscope (node B).

Figure 2 shows the phase ϕ of the optically-carried microwave signal, at point B, versus the diode laser bias current. Tests are performed at a modulation frequency of 10 GHz, for various microwave power values. For all microwave power levels, we observe an absolute phase variation of about 2 rad for a bias current varying from 30 mA to 90 mA. We checked that the measured phase variation is not due to the amplitude modulation-phase modulation (AM-PM) conversion process [40–47] in the photodiode. The contribution of the latter effect is reported on Fig. 2. For this measurement, the laser bias current was fixed to 90 mA. The attenuation of the VOA and the synthesizer microwave power were then adjusted to get optical and microwave powers at the photodiode input comparable to those obtained for standard measurements with bias current values of 30, 50, 70 and 90 mA, and a microwave power of 10 dBm (point A). We note that the AM-PM conversion process measured here is higher than the one reported in Ref. [48], for the same photodiode reference. Our results confirm that the diode laser bias current change is the dominant cause of the observed phase variation.

A network analyzer was also used to measure the S_{21} parameter between the node A, at the microwave input of the diode laser, and the point B', at the output of the fast photodiode. Measurements were carried out in sequence, for bias currents from 15 to 90 mA, in steps of 1 mA. Figure 3 shows the phase ϕ of S_{21} as a function of the bias current for different microwave frequencies.

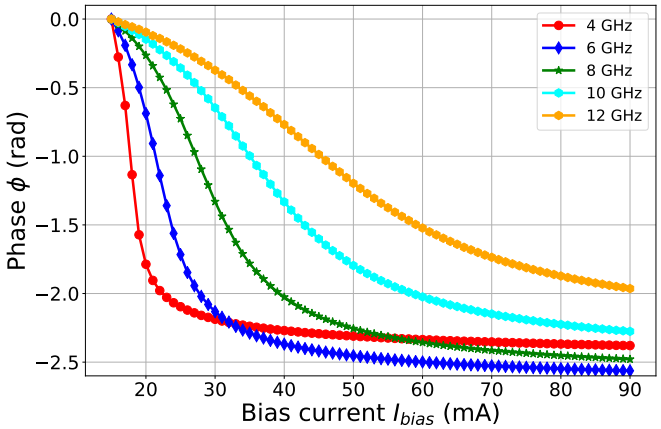

Fig. 3. Phase ϕ of the S_{21} parameter, between the point A and point B′, versus the diode laser bias current for several values of the microwave frequency. The microwave power at the laser input (point A) is 10 dBm. The reference phase value was arbitrarily fixed to 0 for the lowest tested bias current value.

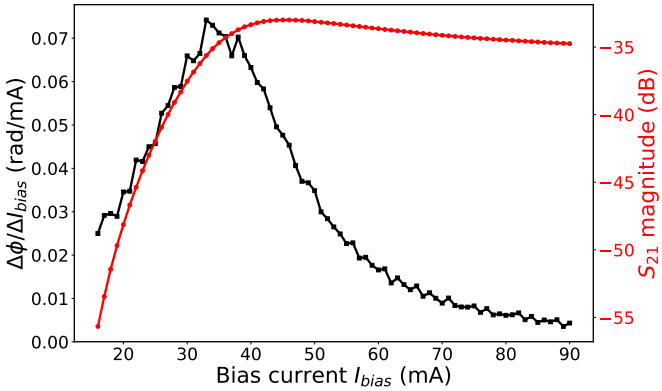

Fig. 4. Current-to-phase sensitivity, in rad/mA, and magnitude of the S_{21} parameter, between points A and B′, versus the bias current, at a microwave frequency of 10 GHz.

For this measurement, the value of the phase ϕ was reinitialized to zero for the lowest tested bias current, The largest variation (2.6 rad on the bias current full range) is obtained at a frequency of 6 GHz. We also note that the slope of the current-to-phase dependence is increased at low bias current frequencies with reduction of the microwave frequency.

Since our goal is to reduce the residual phase noise of the optically-carried microwave signal by acting on the laser bias current while preserving a high dynamic range, a high current-to-phase sensitivity is desired. Also, it is important to ensure that no significant amplitude modulation is produced around this bias point. Extracted from data shown in Fig. 3, Fig. 4 shows the current-to-phase sensitivity and the magnitude of the S_{21} parameter at 10 GHz, versus the laser bias current. We observe that the current-to-phase sensitivity is maximized at a value of about 0.075 rad/mA, for a bias current point of about 35 mA. The S_{21} parameter magnitude curve exhibits an inversion point at a bias current of about 42 mA, around which no significant spurious amplitude modulation should be produced. Note eventually that sensitivities up to 0.2 rad/mA were measured for bias currents of about 15 mA, at 4 GHz.

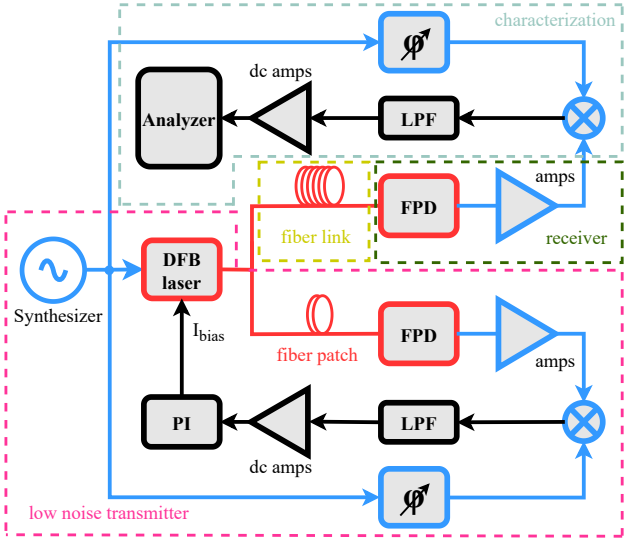

Fig. 5. Experimental setup for residual phase noise and frequency stability measurements at 10 GHz, in free-running or locked modes. The bottom part includes the servo loop. The upper part is an out-of-loop arm used for phase noise or for frequency stability characterization. For phase noise measurement, the analyzer is a FFT analyzer. For frequency stability measurement, the analyzer is a digital voltage multimeter. The color code is red for optics, blue for microwaves and black for dc domains. LPF: low-pass filter. PI: proportional-integral controller.

3. PHASE NOISE AND STABILITY MEASUREMENTS

In this section, we have investigated the possibility to mitigate the residual phase noise at 10 GHz of the modulated-laser system by acting directly on the laser bias current. The setup is shown in Fig. 5. A microwave frequency synthesizer directly modulates the pigtailed laser. The microwave-modulated laser output is split in two subsystems with a fibered coupler. Each subsystem consists of a fiber patch (about 1 meter-long, SMF28 fiber type) terminated by a fast photodiode and microwave amplification (23 dB) for extraction of the optically-carried microwave signal. In the lower subsystem, the 10 GHz signal extracted from the photodetection stage is mixed with the signal from the local synthesizer. This provides at the output of the mixer-based phase detector (Miteq, DBL0218) an error signal that is processed with a proportional-integral (PI) controller to send back corrections to the laser bias current, for compensation of phase fluctuations experienced through the electro-optic conversion process. The second subsystem (upper part of Fig. 5) is used for residual phase noise or stability characterization. The photodetection stage is identical to the one used in the first subsystem. An analyzer, fast-Fourier transform (FFT) for phase noise, or digital voltmeter for stability measurement, is placed, after low-pass filtering, at the mixer output. In the present experiment, fiber patches of both subsystems are not compensated. Note also that if a long-distance microwave transfer had to be implemented with this approach, the long fiber link would replace the patch of the upper subsystem. The subsystem used for the servo part is implemented locally. The experiment was performed at a microwave frequency of 10 GHz, with a bias current of 35 mA, where the current-to-phase sensitivity is maximized (see Fig. 4).

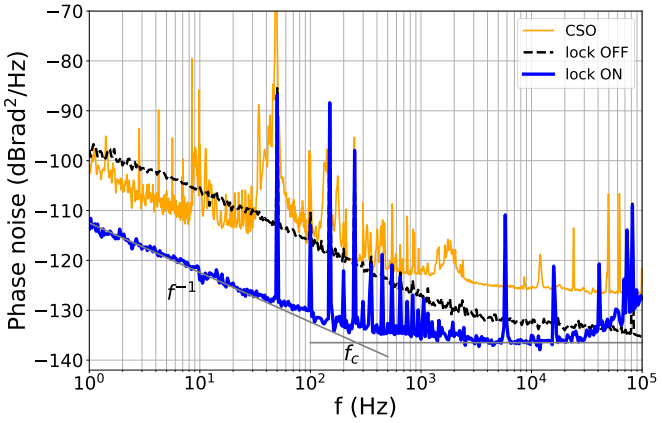

Fig. 6. Residual phase noise at 10 GHz, in free-running mode and locked modes, for a bias current of 35 mA. The absolute phase noise of a CSO developed in the laboratory is shown for comparison.

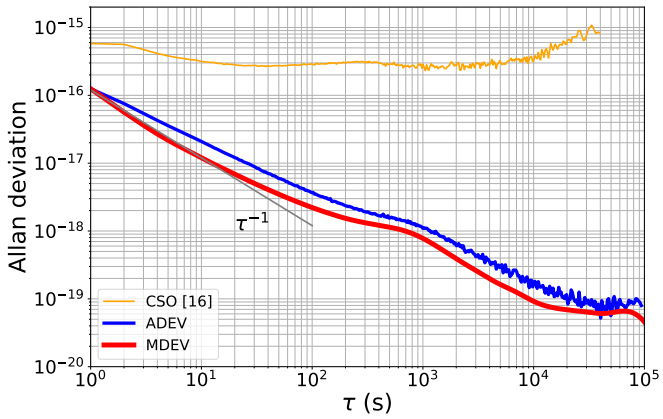

Fig. 7. Allan deviation of the modulated-laser system, with active servo on the laser bias current. Standard and modified Allan deviation are reported. The Allan deviation (drift-removed) of a CSO [16] is also shown for comparison. The measurement cutoff frequency is f_H = 10 Hz.

Figure 6 shows residual phase noise results of the modulated-laser system, with or without activation of the laser current lock. In the free-running case, the phase noise is about −97, −127 and − 136 dBrad^2/Hz at 1 Hz, 1 kHz and 100 kHz offset frequencies, respectively. In the locked case, the residual phase noise is reduced by more than 10 dB in the 1 Hz - 1 kHz range, yielding −113 dBrad^2/Hz at f = 1 Hz. Since this measurement includes the contribution of two nearly-identical detection stages, the residual phase noise for a single-arm system is about −116 dBrad^2/Hz at f = 1 Hz. We found that the residual phase noise of the microwave amplifiers of the photodetection stage limits the residual phase noise of the system [17]. For Fourier frequencies f lower than the cutoff frequency $f_c \simeq 230$ Hz, the spectrum exhibits a $1/f$ flicker phase noise slope. Describing the phase noise spectrum by the power-law $S_\phi(f) = b_{-1}/f + b_0$, with $b_0 = -136$ dBrad^2/Hz and $b_{-1} = -113$ dBrad^2, the predicted Allan deviation σ_y (τ = 1 s) = $\sqrt{\sigma_{fpn}^2 + \sigma_{wpn}^2}$, with $\sigma_{fpn}^2 = [0.166 + \frac{3\ln f_H}{4\pi^2}]\frac{h_1}{\tau^2}$, $\sigma_{wpn}^2 = \frac{3f_H}{4\pi^2}\frac{h_2}{\tau^2}$, $h_1 = \frac{b_{-1}}{\nu_0^2}$, $h_2 = \frac{b_0}{\nu_0^2}$, f_H = 10 Hz the measurement cutoff frequency [49], and ν_0 the carrier frequency (10 GHz), is about 1.3×10^{-16}. In this test, the servo bandwidth is higher than 100 kHz, allowing to obtain, in comparison with the free-running case, improved performances for offset frequencies lower than 40 kHz. We also plot in Fig. 6 the absolute phase noise of a CSO. For this measurement, the signal of a first CSO was injected in the laser system, extracted at the photodetection stage output, and then compared to a second CSO using a noise analyzer. Without activation of the current servo, the phase noise of the CSO is clearly, in some regions, lower than the system residual phase noise, meaning that the CSO could not be disseminated without degradation. With activation of the current servo, the system exhibits a residual phase noise well lower than the CSO phase noise. In this case, the CSO microwave signal can be transferred without degradation.

Finally, we have measured the Allan deviation of the modulated-laser system in locked conditions. For this purpose, the analyzer shown in Fig. 5 is a digital voltage multimeter. Acquired voltage data are converted through the mixer sensitivity into phase data, from which frequency data are derived to extract Allan deviation results, shown in Fig. 7. The Allan deviation is 1.2×10^{-16} at 1 s, in good agreement with the value (1.3×10^{-16}) predicted from the residual phase noise measurement. Since the measurement shown in Fig. 7 includes two detection stages, the fractional frequency stability at 1 s of a single arm is expected to be $1.2 \times 10^{-16}/\sqrt{2} \simeq 9 \times 10^{-17}$. For integration times from 1 s to 10 s, the modified Allan deviation (MDEV) slope fits the ideally-expected $1/\tau$ slope. For $\tau > 10$ s, the Allan deviation slope is reduced. This is ascribed to thermal effects or various perturbations along the non-compensated fiber path. A bump is observed on the curve at about 800 s, probably induced by the lab air conditioning system. The residual fractional frequency stability, obtained for two systems, is of 1.8×10^{-19} and 9×10^{-20} at 10^4 and 10^5 s, respectively. This level is well-below the instability level of the CSO and demonstrates that our system is able, with activation of the current servo, to transmit the CSO signal without stability degradation.

4. CONCLUSIONS

We have proposed a simple approach for mitigating the residual phase noise of a microwave current-modulated laser system. In this method, an error signal, image of the phase difference between the driving microwave source and the photonically-extracted microwave signal at the output of the photodetection stage, is used to actively control the laser bias current in a feedback servo loop. We have investigated the current-to-phase dependence of the laser system at several microwave frequencies and powers, in order to identify optimal bias current operation points. Sensitivities up to 0.2 rad/mA were measured at low frequencies and low bias current values. We have checked that the impact of the bias current change was the dominant contribution to the observed phase variation and that the latter was not due to the AM-PM conversion in the photodiode. With this technique, we have demonstrated, with a bias current of 35 mA, a residual phase noise reduction at 10 GHz by more than 10 dB in the 1 Hz - 1 kHz range, yielding the level of −113 dBrad^2/Hz at 1 Hz offset frequency. The residual Allan deviation of the system is measured to be 1.2×10^{-16} at 1 s and below 1×10^{-19} at 10^5 s. These performances exceed the needs required for the distribution of the most stable microwave signals delivered by cryogenic sapphire oscillators or frequency-divided cavity-stabilized lasers, in a simple photonic architecture.

FUNDING

This work has been partly funded by Région Bourgogne Franche-Comté with the HACES project (grant 2018-04768), and by Agence Nationale de la Recherche (ANR) in the frame of the LabeX FIRST-TF (Grant ANR 10-LABX-0048), EquipeX Oscillator-IMP (Grant ANR 11-EQPX-0033), and EIPHI Graduate school (Grant ANR-17-EURE-0002) projects.

ACKNOWLEDGMENTS

The authors would like to thank Vincent Giordano (FEMTO-ST), Enrico Rubiola (FEMTO-ST and INRIM), and Claudio Calosso (INRIM), for fruitful discussions and reading of the manuscript. The authors also thank A. L. Billabert (ESYCOM) for providing us information and references about the noise modeling of semiconductor lasers.

DISCLOSURES

The authors declare no conflicts of interest.

DATA AVAILABILITY STATEMENT

The data that support the findings of this study are available from the corresponding author upon reasonable request.

REFERENCES

1. P. Ghelfi, F. Laghezza, F. Scotti, G. Serafino, A. Capria, S. Pinna, D. Onori, C. Porzi, M. Scaffardi, A. Malacarne, V.Vercesi, E. Lazzeri, F. Berizzi, and A. Bogoni, A fully photonics-based coherent radar system, Nature **507,** 7492, 341-345 (2014).
2. S. Koenig, D. Lopez-Diaz, J. Antes, F. Boes, R. Henneberger, A. Leuther, A. Tessmann, R. Schmogrow, D. Hillerkuss, R. Palmer, T. Zwick, C. Koos, W. Freude, O. Ambacher, J. Leuthold, and I. Kallfass, Wireless sub-THz communication system with high data rate, Nat. Photonics **7,** 977-981 (2013).
3. G. Santarelli, Ph. Laurent, P. Lemonde, A. Clairon, A. G. Mann, S. Chang, A. N. Luiten, and C. Salomon, Quantum projection noise in an atomic fountain, Phys. Rev. Lett. **82,** 4619 (1999).
4. T. Nakamura, J. Davila-Rodriguez, H. Leopardi, J. A. Sherman, T. M. Fortier, X. Xie, J. C. Campbell, W. F. McGrew, X. Zhang, Y. S. Hassan, D. Nicolodi, K. Beloy, A. D. Ludlow, S. A. Diddams, and F. Quinlan, Coherent optical clock down-conversion for microwave frequencies with 10^{-18} instability, Science **368,** 6493, 889-892 (2020).
5. G. C. Valley, Photonic analog-to-digital converters, Opt. Exp. **15,** 5, 1955-1982 (2007).
6. N. Nand, J. Hartnett, E. Ivanov, and G. Santarelli, Ultra-stable very-low phase-noise signal source for very long baseline interferometry using a cryocooled sapphire oscillator, IEEE Trans. Microwave Theory Techn. **59,** 11, 2978-2986 (2011).
7. B. Francois, C. E. Calosso, M. Abdel Hafiz, S. Micalizio and R. Boudot, Simple-design ultra-low phase noise microwave frequency synthesizers for highperforming Cs and Rb vapor-cell atomic clocks, Rev. Sci. Instr. **86,** 094707 (2015).
8. E. N. Ivanov and M. E. Tobar, Low phase-noise microwave oscillators with interferometric signal processing, IEEE Trans. Microwave Theory Tech. **54,** 8, 3284-3294 (2006).
9. E. N. Ivanov and M. E. Tobar, Low phase-noise sapphire crystal microwave oscillators: current status, IEEE Trans. Ultrason. Ferroelec. Freq. Contr. **56,** 2, 263-269420 (2009).
10. L. Maleki, The optoelectronic oscillator. Nat. Photonics **5,** 728 (2011).
11. B. Sinquin, M. Romanelli, S. Bouhier, L. Frein, M. Alouini and M. Vallet, Low phase noise direct-modulation optoelectronic oscillator, J. Light. Technol. **39,** 7788 (2021).
12. J. Li, H. Lee, and K. Vahala, Microwave synthesizer using an on-chip Brillouin oscillator, Nature Comm. **4,** 2097 (2013).
13. C. L. Degen, F. Reinhard, P. Cappellaro, Quantum sensing, Rev. Mod. Phys. **89,** 035002 (2017).
14. S. Grop, P.-Y. Bourgeois, R. Boudot, Y. Kersalé, E. Rubiola, and V. Giordano, 10 GHz cryocooled saphhire oscillator with extremely low phase noise, Electron. Lett. **46,** 420 (2010).
15. J. G. Hartnett, Ultra-low-phase-noise cryocooled microwave dielectric-sapphire-resonator oscillators, Appl. Phys. Lett. **100,** 183501 (2012).
16. C. Fluhr, S. Grop, B. Dubois, Y. Kersalé, E. Rubiola and V. Giordano, Characterization of the individual short-term frequency stability of cryogenic sapphire oscillators at the 10^{-16} level, IEEE Trans. Ultrason. Ferroelec. Freq. Contr. **63,** 6, 915-922 (2016).
17. R. Boudot and E. Rubiola, Phase noise in RF and microwave amplifiers, IEEE Trans. Ultrason. Ferroelec. Freq. Contr. **59,** 12, 2613-2624 (2012).
18. T. M. Fortier, M. S. Kirchner, F. Quinlan, J. Taylor, J. C. Bergquist, T. Rosenband, N. Lemke, A. Ludlow, Y. Jiang, C. W. Oates, and S. A. Diddams, Generation of ultrastable microwaves via optical frequency division, Nat. Photonics **5,** 425 (2011).
19. X. Xie, R. Bouchand, D. Nicolodi, M. Giunta, W. Hänsel, M. Lezius, A. Joshi, S. Datta, C. Alexandre, M. Lours, P.-A. Tremblin, G. Santarelli, R. Holzwarth, and Y. Le Coq, "Photonic microwave signals with zeptosecond-level absolute timing noise," Nat. Photonics **11,** 44-47 (2017).
20. M. Giunta, J. Yu, M. Lessing, M. Fischer, M. Lezius, X. Xie, G. Santarelli, Y. Le Coq, and R. Holzwarth, Compact and ultrastable photonic microwave oscillator, Opt. Lett. **45,** 1140-1143 (2020).
21. N. V. Nardelli, T. M. Fortier, M. Pomponio, E. Baumann, C. Nelson, T. R. Schibli and A. Hati, 10 GHz generation with ultra-low phase noise via the transfer oscillator technique, APL Photonics **7,** 026105 (2022).
22. P. Brochard, S. Schilt, and T. Südmeyer, Ultra-low noise microwave generation with a free-running optical frequency comb transfer oscillator, Opt. Lett. **43,** 19, 4651-4654 (2018).
23. M.Kalubovilage, M. Endo and T. R. Schibli, Ultra-low phase noise microwave generation with a free-running monolithic femtosecond laser, Opt. Exp. **28,** 17, 25400-25409 (2020).
24. A. L. Gaeta, M. Lipson, and T. J. Kippenberg, Photonic-chip-based frequency combs, Nat. Photonics **13,** 158-169 (2019).
25. J. Liu, E. Lucas, A. S. Raja, J. He, J. Riemensberger, R. N. Wang, M. Karpov, H. Guo, R. Bouchand, and T. J. Kippenberg, Photonic microwave generation in the X- and K-band using integrated soliton microcombs, Nat. Photonics **14,** 8, 486-491 (2020).
26. S. Droste, F. Ozimek, Th. Udem, K. Predehl, T. W. Hänsch, H. Schnatz, G. Grosche and R. Holzwarth, Optical-frequency transfer over a single-span 1840 km fiber link, Phys. Rev. Lett. **111,** 110801 (2013).
27. K. Predehl, G. Grosche, S. M. F. Raupach, S. Droste, O. Terra, J. Almis, Th. Legero, T. W. Hänsch, Th. Udem, R. Holzwarth and H. Schnatz, A 920-kilometer optical fiber link for frequency metrology at the 19^{th} decimal place, Science **336,** 441 (2016).
28. J. Grotti, S. Koller, S. Vogt, S. Häfner, U. Sterr, C. Lisdat, H. Denker, C. Voigt, L. Timmen, A. Rolland, F. N. Baynes, H. S. Margolis, M. Zampaolo, P. Thoumany, M. Pizzocaro, B. Rauf, F. Bregolin, A. Tampellini, P. Barbieri, M. Zucco, G. A. Costanzo, C. Clivati, F. Levi, and D. Calonico, Geodesy and metrology with a transportable optical clock, Nat. Phys. **14,** 437-441 (2018).
29. C. Daussy, O. Lopez, A. Amy-Klein, A. Goncharov, M. Guinet and C. Chardonnet, Long-distance frequency dissemination with resolution of 10^{-17}, Phys. Rev. Lett. **94,** 203904 (2005).
30. S. M. Foreman, K. W. Holman, D. D. Hudson, D. J. Jones and J. Ye, Remote transfer of ultrastable frequency references via fiber networks, Rev. Sci. Instrum. **78,** 021101 (2007).
31. O. Lopez, A. Amy-Klein, M. Lours, C. Chardonnet and G. Santarelli, High-resolution microwave frequency dissemination on an 86-km urban optical link, Appl. Phys. B **98,** 723 (2010).

32. O. Lopez, A. Kanj, P-E. Pottie, D. Rovera, J. Achkar, C. Chardonnet, A. Amy-Klein and G. Santarelli, Simultaneous remote transfer of accurate timing and optical frequency over a public fiber network, Appl. Phys. B **110,** 3 (2013).
33. S. Wang, D. Sun, Y. Dong, W. Xie, H. Shi, L. Yi and W. Hu, Distribution of high-stability 10 GHz local oscillator over 100 km optical fiber with accurate phase-correction system, Opt. Lett. **39,** 888 (2014).
34. H. Quan, W. Xue, W. Zhao, Y. Xing, H. Jiang, W. Guo and S. Zhang, Microwave frequency dissemination over a 212 km cascaded urban fiber link with stability at the 10^{-18} level, MDPI Photonics **9,** 399 (2022).
35. F. Narbonneau, M. Lours, S. Bize, A. Clairon, G. Santarelli, O. Lopez, C. Daussy, A. Amy-Klein and C. Chardonnet, High resolution frequency standard dissemination via optical fiber metropolitan network, Rev. Sci. Instrum. **77,** 064701 (2006).
36. A. Bdeoui, A. L. Billabert, N. Breuil and C. Rumerlhard, Direct modulation of a laser by a microwave signal: A model for $1/f$ amplitude and phase noises, Proceedings 33rd European Microwave Conference, Munich, Germany, 1409-1412 (2003).
37. W-E. Kassa, A-L. Billabert, S. Faci and C. Algani, Electrical modeling of semiconductor laser diode for heterodyne RoF system simulation, IEEE J. Quant. Elec. **49,** 10, 894-900 (2013).
38. M. Ahmed, M. Yamada and M. Saito, Numerical modeling of intensity and phase noise in semiconductor lasers, IEEE J. Quant. Elec. **37,** 12, 1600-1610 (2001).
39. K. G. Libbrecht and J. L. Hall, A low-noise high-speed diode laser current controller, Rev. Sci. Instrum. **64,** 2133 (1993).
40. E. N. Ivanov, S. A. Diddams and L. Hollberg, Study of the excess noise associated with demodulation of ultra-short infrared pulses, IEEE Trans. Ultrason. Ferroelec. Freq. Contr. **52,** 1068 (2005).
41. M. Currie and I. Vurgaftman, Microwave phase retardation in saturated InGaAs photodetectors, IEEE Photonics Technol. Lett. **18,** 1433 (2006).
42. J. Taylor, S. Datta, A. Hati, C. Nelson, F. Quinlan, A. Joshi and S. Diddams, Characterization of power-to-phase conversion in high-speed P-I-N photodiodes, IEEE Photonics J. **3,** 140 (2011).
43. W. Zhang, T. Li, M. Lours, S. Seidelin, G. Santarelli, and Y. Le Coq, Amplitude to phase conversion of InGaAs pin photodiodes for femtosecond lasers microwave signal generation, Appl. Phys. B **106,** 2, 301-308 (2012).
44. T. M. Fortier, F. Quinlan, A. Hati, C. Nelson, J. A. Taylor, Y. Fu, J. Campbell, and S. A. Diddams, Photonic microwave generation with high-power photodiodes, Opt. Lett. **38,** 1712-1714 (2013).
45. D. H. Phung, M. Merzougui, C. Alexandre and M. Lintz, Phase measurement of a microwave optical modulation : characterisation and reduction of amplitude-to-phase conversion in 1.5 μm high bandwidth photodiodes, J. Light. Technol. **32,** 3579 (2014).
46. A. Beling, X. Xie, and J. C. Campbell, High-power, high-linearity photodiodes, Optica **3,** 3, 328-338 (2016).
47. L. Kang and B. H. Kolner, Characterization of AM-PM conversion in silicon p-i-n photodiodes, IEEE Photonics Technol. Lett. **31,** 1001 (2019).
48. D. Eliyahu, D. Seidel and L. Maketi, RF amplitude and phase-noise reduction of an optical link and an opto-electronic oscillator, IEEE Trans. Microw. Theory Techn. **56,** 449 (2008).
49. E. Rubiola and F. Vernotte, The companion of the Enrico's chart for phase noise and two-sample variances, ArXiV:2201.07109v2 (2022).